An approach to seismic damage detection and evaluation in RC bridge piers through vibration data

Alessandro Lubrano Lobianco [a]*, Marta Del Zoppo[a], Carlo Rainieri[b], Giovanni Fabbrocino[b,c], Marco Di Ludovico[a]

[a]*Department of Structural Engineering and Architecture, University of Naples "Federico II", Naples (IT)*

[b]*ITC-CNR, Institute for Construction Technologies, Italian National Research Council (IT)*

[c]*Department of Biosciences and Territory, University of Molise, Campobasso (IT)*

*corresponding author: alessandro.lubranolobianco@unina.it

An approach to seismic damage detection and evaluation in RC bridge piers through vibration data

A timely post-earthquake damage evaluation in existing bridges is fundamental for an efficient emergency management. Structural Health Monitoring (SHM) systems can allow a fast damage assessment; however, a lack of methods for the SHM data interpretation is recognised. The present paper proposes an approach for the probabilistic seismic damage detection and quantification in ductile bridge piers from vibration-based SHM data by comparing time variations of modal properties. To this aim, the selected modal properties are natural frequencies and mode-shapes, expressed in terms of CoMAC and ECoMAC indices. Experimental results of quasi-static cyclic tests and output-only modal identification tests are adopted to calibrate a reliable finite element model able to predict the variations in fundamental modal properties of ductile RC piers due to seismic damage. The calibrated model is used to perform probabilistic analyses to derive probability distributions for the variation of the considered modal-based features of piers at different seismic damage levels. The approach provides fragility models to support a timely assessment of serviceability levels in monitored assets in the immediate aftermath of an earthquake by monitoring the variation of natural frequencies. Conversely, CoMAC and ECoMAC resulted slightly sensitive to seismic damage for the investigated piers portfolio.

Keywords: Modal-based damage evaluation; measure of damage; degrading structures fundamental frequency; Coordinate Modal Assurance Criterion; simply supported bridges; Structural Health Monitoring; Operational Modal Analysis.

1. Introduction

Bridges are critical components of transportation infrastructure networks, and unattended damage or degradation phenomena can result in severe economic losses as well as consequences on public safety. In order to ensure that bridges are able to sustain

design loads (dead and live loads as well as extreme ones, such as those generated by earthquakes) over their lifetime, appropriate maintenance to ensure structural integrity is required. The latter is typically evaluated by means of regular visual inspections carried out by appropriately trained experts. Results of inspections are usually collected into Bridge Management Systems (BMS) and used to make informed decisions regarding intervention strategies (Hurt & Schrock, 2016). Such information can be complemented by detailed physical and mechanical measures taken according to the Structural Health Monitoring (SHM) paradigm (Ministero delle Infrastrutture e dei Trasporti & Consiglio Superiore Lavori Pubblici, 2020). The recent advances in SHM make possible the remote assessment of the performance and health condition of structures under service loads (traffic, wind, temperature, and so on) as well as exceptional loads, such as earthquakes, at the expenses of a moderate financial investment in measurement equipment and data processing software. Compared to traditional visual inspections, SHM offers attractive advantages, such as timely and remote detection of incipient damage conditions and detection of hidden damage (e.g., possible cracks caused by an earthquake in the core concrete of columns in retrofitted bridges which are hidden by their jackets; see Mirza, 2006). Furthermore, being the structural health assessment based on quantitative SHM data, the influence of subjectivity of the expert judgement is avoided. Timely detection of degradation phenomena from SHM data can provide a valuable contribution to shift the maintenance paradigm for bridges from scheduled (time based) to proactive (condition based) maintenance (Rainieri et al., 2020). In addition, SHM systems in earthquake prone regions can provide significant information to remotely assess the health condition and serviceability of bridges immediately after the occurrence of a seismic event, and support emergency management and quick decision making to reduce the risk of secondary losses (Mirza, 2006). When vibration based SHM of bridges is

considered, modal properties are used as damage features either directly or in the form of derived quantities, such as modal strain energy, mode shape curvature, dynamic flexibility, etc. (Limongelli & Giordano, 2020). Natural frequencies have been extensively used for vibration-based SHM of bridges (Jin et al., 2016; Junwon et al., 2015; Kariyawasam et al., 2020) because they can be more easily and accurately measured than other modal-based damage sensitive features. Natural frequencies are effective in damage detection, but they have limited reliability for damage location. To overcome such limitation, damage features based on mode shapes are particularly attractive holding spatial information exploitable for damage localization. The first attempts of using mode shapes as damage sensitive features relied on the evaluation of the Modal Assurance Criterion (MAC) (Allemang & Brown, 1982) between couples of corresponding modes before and after damage occurrence. However, the MAC index is not very sensitive to local deviations of modal displacements (Foti, 2013) and to small changes or small magnitude of modal displacements (Rainieri & Fabbrocino, 2014); so, the Coordinate Modal Assurance Criterion (CoMAC) has been introduced as an alternative (Lieven & Elwins, 1988, Rainieri & Fabbrocino, 2014). Applications of MAC and CoMAC to damage detection in bridge structures revealed that they can detect most structural changes and locations, but also identify spurious damage (Moughty & Casas, 2017). Even if CoMAC may yield false damage detections, it is still widely applied to SHM of bridges, sometimes in combination with other methodologies to improve its performance (Moughty & Casas, 2017). The Enhanced Coordinate Modal Assurance Criterion (ECOMAC) basically represents a measure of the average difference between the vector components corresponding to a certain degree of freedom (DOF) and it has been proposed to overcome the potential problems caused by erroneous scaling (Hunt 1992).

The recent literature explores the development of fragility models based on damage features extracted from permanent vibration-based monitoring systems for the seismic damage assessment of structures. Reuland et al. (2023) and Martakis et al. (2023) investigated the use of data-driven techniques derived from vibration monitoring for the damage assessment of masonry buildings.

The literature review points out two main challenges in the application of damage assessment techniques from vibration-based SHM data to bridges. The first concerns the limited availability of monitoring data over wide time scales holding information about damage effects on dynamic properties under varying environmental/operational conditions to be used as a reference for damage detection and quantification. The second challenge concerns the possibility of exploiting modal properties to get quantitative information about the structural performance and safety of the monitored bridge (Mirza, 2006). This aspect, rarely addressed by the scientific community, is of particular interest for SHM applications in earthquake prone regions (Zhelyazkov et al., 2020), when prompt serviceability assessment of bridges hit by an earthquake might be critical for emergency management and shortening down-time implies significant economic savings. In this framework, the present paper aims at tackling the problem of the correlation between information on modal properties variation derived from SHM data and actual damage levels occurred in the monitored bridges after an earthquake. The study focuses on a specific class of bridges, the simply supported Reinforced Concrete (RC) bridges, which represents a very common typology of existing road bridges. Among the failure modes affecting this specific bridge type under seismic excitation, those related to flexural and shear capacity of piers play a relevant role due to different reasons (inadequate flexural strength or ductility, inadequate splice length, inadequate transverse reinforcement, etc.). Thus, the study focuses on the performance of ductile piers governed

by a flexural failure mode. In such a context, the response of the structure is governed by fundamental frequencies depending on the mass of the decks and on the stiffness of the piers (Priestley, M.J.N., Seible F., Calvi, 1996). The structural damage can be detected, in principle, by focusing on the vibration response of piers only, so the number of sensors to install and the cost of the monitoring system can be optimized by limiting the observability to those primary structural elements. The significance of monitoring the acceleration response of piers for the selected class of bridges is confirmed by a number of applications (Londono, 2006; Moroni et al., 2005; Rainieri et al., 2018). In particular, the measured acceleration response of the piers can be processed in order to perform reliable estimates of its dynamic properties that can be effectively used to assess the structural integrity (Fujino & Siringoringo, 2008; Jr et al., 2006). Following these results, this study investigates through numerical simulations the influence of different seismic damage scenarios on the dynamic response of a portfolio of ductile RC piers whose geometrical and mechanical properties are based on real surveys carried out on existing Italian RC bridges of the simply supported type. The study consists of three main sections focussing on: *i)* damage estimation analysis by means of literature approaches; *ii)* experimental testing to simulate seismic damage on RC piers and calibration of a reliable Finite Element (FE) model; *iii)* development of a correlation tool between modal-based damage features and seismic damage levels. In particular, the first section summarizes the approach adopted to correlate selected damage features with the seismic damage level affecting the monitored bridge pier. The second section describes the experimental tests carried out to establish a correlation between selected simulated seismic damage and the resulting fundamental modal properties of the piers; the experimental results from quasi-static cyclic tests and output-only modal identification are used to calibrate a refined FE model. Starting from the refined FE model, the last section adopts the proposed approach

to correlate in a probabilistic framework the variation of modal properties with defined damage levels for a portfolio of existing RC bridge piers. The analysis allows to investigate the sensitivity of the selected modal properties to the structural damage level occurred in the piers, accounting for uncertainties related to geometry and mechanical properties. The derived fragility model provides a quantitative information about the structural performance and safety of piers by processing SHM data in the immediate aftermath of an earthquake.

2. Damage estimation

The present study adopts a probabilistic framework to investigate the correlation between seismic damage level and variations in modal properties of ductile RC piers through numerical simulations. Potentialities and issues of exploiting different modal-based damage features to get quantitative information about the structural damage and safety level of monitored bridges are investigated. In detail, the considered damage features are the fundamental frequency and the CoMAC (or its enhanced version, ECoMAC) (Rainieri & Fabbrocino, 2014). For the seismic damage quantification, the damage scale proposed by Park and Ang (1985) is adopted, given its wide application for the seismic damage assessment in existing structures (Table 1). The Park and Ang (P&A) damage classification correlates the damage level experienced during a seismic event with the reparability of a structure and considers five damage levels from slight to complete. The achievement of each damage level can be quantitatively assessed through a Damage Index (DI) accounting both for energy dissipation and ductility demand, as:

ha eliminato: Table 1

ha formattato: Tipo di carattere: 12 pt

$$DI = \frac{\delta_m}{\delta_u} + \frac{\beta}{Q_y \delta_u} \int_0^t dE \quad (1)$$

where δ_m is the maximum deformation demand, δ_u is an ultimate deformation capacity, Q_y is the calculated yield strength and dE is the incremental hysteretic energy (demand). The constant parameter β gives the ratio of incremental damage caused by an increase of the maximum response to the normalized incremental hysteretic energy, taken equal to 0.25 for slightly reinforced members (Promis et al., 2009).

Table 1 - Seismic damage scale from Park and Ang (1985)

Park&Ang Damage Index	Damage level	Repairability	Damage state (DS)
DI < 0.10	No or slight damage	Repairable damage	DS0
0.10 ≤ DI ≤ 0.25	Minor damage	Repairable damage	DS1
0.25 < DI ≤ 0.4	Moderate damage	Repairable damage	DS2
0.4 < DI < 0.80	Severe damage	Irrepairable damage	DS3
DI ≥ 0.80	Complete damage	Irrepairable damage	DS4

Experimental tests on two cantilever RC columns governed by a flexural failure mode are performed to assess the influence of the seismic damage on selected damage features for column-type structural members, like piers. Both quasi-static testing and output-only modal identification tests are performed. The experimental results from the two tested specimens and from six additional tests taken from the literature are used for the calibration and validation of a FE model able to simulate the effect of seismic damage occurred in column-type members on the dynamic response at low amplitude vibrations. The refined FE model is then used to perform probabilistic analyses aimed at defining, through numerical simulations on a portfolio of 200 rectangular RC piers subjected to seismic excitation of six different intensities, probability distributions for the variation of

selected damage features in relation to the P&A damage scale to provide an immediate quantification of the occurred damage. It is worth noting that the adopted numerical model can provide an approximation of the real seismic response of the bridge prototype as long as the bridge is straight and consists of a large number of equal spans and piers of equal height or stiffness (Priestley, M.J.N., Seible F., Calvi, 1996). The assessment of the role of environmental variables, such as temperature, on modal properties of the piers is out of the scope of the present paper; thus, it is not considered in this study. However, several procedures to compensate their effects are available in the literature (Rainieri et al., 2019; Reynders et al., 2014). Hence the attention can be focused on the magnitude of damage-induced variations of natural frequencies without prejudice for the practical SHM applications (Magalhães et al., 2012). Furthermore, it is assumed that the dynamic performance of the pier in the reference condition before the earthquake is accurately characterized, so that attention can be focused on the effect of seismic damage only. Details about the experimental tests, model calibration, and simulations for a probabilistic damage quantification are discussed in the following sections.

3. Seismic damage simulation: experimental testing

The structural damage induced by seismic excitation is experimentally simulated on two identical RC columns governed by a flexural behaviour. The specimens (termed A and B) are cantilever columns with a rectangular cross section (300x500 mm^2) and are reinforced with 12 ϕ12 smooth steel rebars, as shown in Figure 1. Mechanical properties of materials derived from experimental testing on cubic concrete specimens and steel bars samples. The mean concrete compressive strength of the specimens at the time of testing is 28.8 MPa; the steel mean yielding strength is 330 MPa.

ha eliminato: Figure 1

ha formattato: Tipo di carattere: 12 pt

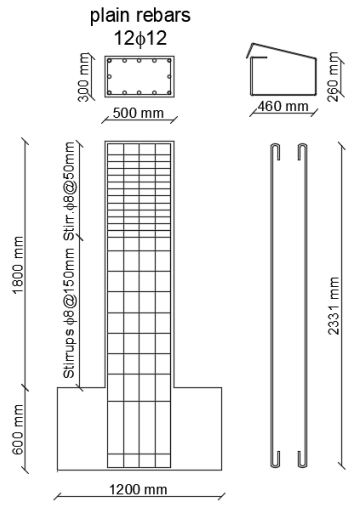

Figure 1. Geometry and reinforcement details of the tested specimens (A and B), dimensions in mm

Specimen A is damaged along its strong direction while specimen B is damaged along its weak direction. Three different damage configurations are simulated, where C_0 represents the undamaged configuration for both specimens (A and B); C_1 and C_2 are representative of a moderate seismic damage for a seismic loading along the strong (specimen A) and weak (specimen B) direction of the column.

3.1 Quasi-static cyclic tests

Seismic damage is simulated through quasi-static cyclic testing. The experimental tests are carried out under displacement control imposing cyclic displacements at the top of the specimen along the strong or the weak axis of the rectangular column, respectively. The horizontal axis of the actuator, shown in Figure 2(a), is located at a distance of 1500 mm from the base of the column. Both specimens A and B are pushed up to a drift ratio (DR, ratio between top displacement and column height) of 1.6%, according to the load

ha eliminato: Figure 2

protocol shown in Figure 2(b). The specimens are subjected to a constant axial load equal to 428 kN, corresponding to a dimensionless axial load ratio ν of 0.1. A more detailed description of the setup and instrumentation can be found in Di Ludovico et al. (2014) and in Del Zoppo et al. (2018), and are not reported herein for the sake of brevity.

ha eliminato: Figure 2

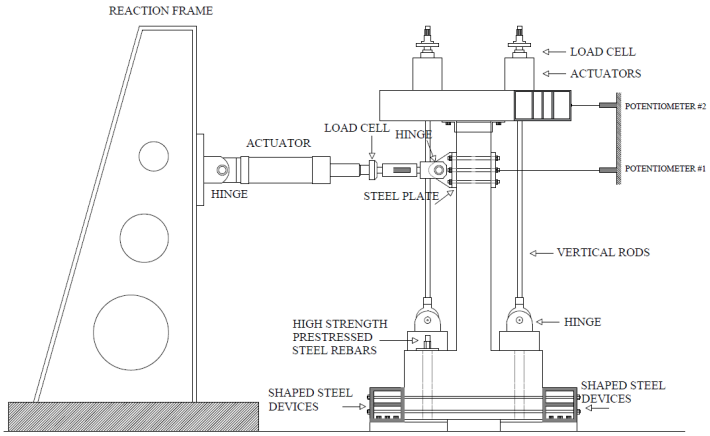

a)

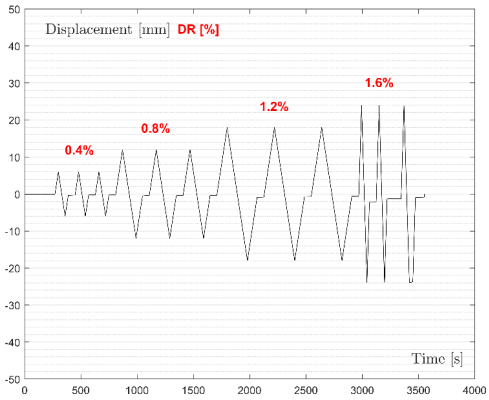

b)

Figure 2. Experimental setup for the quasi-static cyclic loading tests (a) and displacement loading sequence (b).

Specimen A, damaged along its strong direction, experienced a P&A DI of 0.334 for a DR of 1.6%; similarly, specimen B achieved a DI of 0.336 along its weak direction for a DR of 1.6%. Hence, both specimens are representative of a moderate seismic damage condition (i.e., DS2) according to the damage level classification reported in Table 1. Capacity curves of both specimens are shown in Figure 3. Both specimens reached the yielding of internal steel rebars, as visible from the capacity curves. At the end of the tests, the specimens showed only hairline cracks on the concrete cover.

ha eliminato: Table 1

ha eliminato: Figure 3

ha formattato: Tipo di carattere: 12 pt

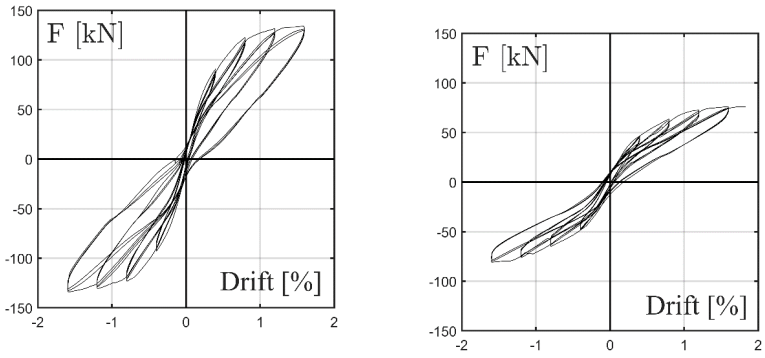

a) b)

Figure 3. Experimental seismic damage simulation: configurations C_1 (a) and C_2 (b).

3.2 Output-only modal identification tests

Output-only modal identification tests have been carried out on the specimens before and after the quasi-static cyclic testing to experimentally assess the influence of damage on the modal properties of the structural members, and to obtain experimental results exploitable for model calibration and validation. Before performing the output-only modal identification tests, the set-up instrumentation for cyclic testing (i.e., actuator and jacks) was removed to avoid any interference with the modal properties of the cantilever columns. Four uniaxial piezoelectric accelerometers (10 V/g sensitivity, ±0.5 g full-scale range, 0.000008 g rms resolution) were installed along the strong as well as weak direction of the columns at different locations (600 mm, 900 mm, 1200 mm and 1500 mm from the column base) (Figure 4). The layout and position of the accelerometers have been defined based on the numerical mode shapes of the cantilever columns. Signals were acquired by a 24-bit digitizer equipped with analog anti-aliasing filter and sampled at 200 Hz. The adopted sampling frequency was sufficient to ensure the identification of the fundamental frequency in each direction. In order to enhance the signal-to-noise ratio, the columns were randomly (spatially and temporally) excited during the tests (Brincker & Ventura, 2015).

ha eliminato: Figure 4

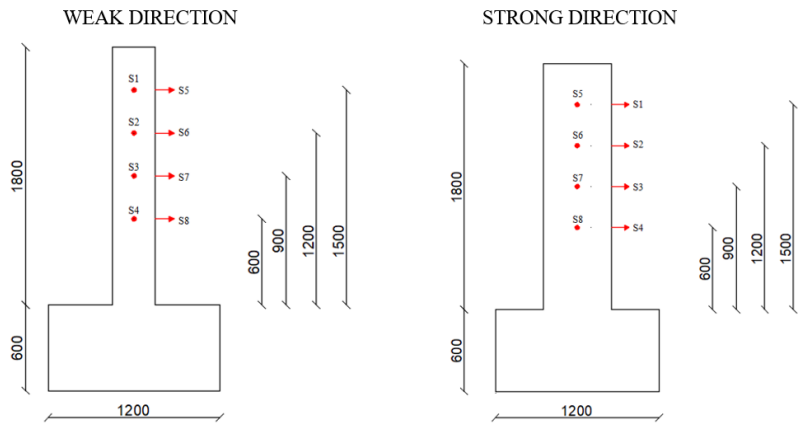

Figure 4. Uniaxial piezoelectric accelerometers layout for OMA tests in the strong (sensors S1 to S4) and weak direction (sensors 5 to 8), dimensions in mm.

The collected data have been processed according to the Basic Frequency Domain method (Rainieri & Fabbrocino, 2014), also known as peak picking method, since closely spaced modes were not expected. The frequency resolution in Power Spectral Density (PSD) estimation was 0.1 Hz. PSDs have been computed according to the Welch's method by applying 50% overlap and Hanning window. The natural frequencies in the strong and weak directions of the tested specimens in the undamaged and damaged configuration are summarized in Table 2. Output-only modal identification test results on the undamaged configuration are available only for specimen B due to acquisition issues during the test on specimen A. However, being the specimens identical in geometry, mechanical properties, casting and curing procedures, and base constrain, the values reported in Table 2 for the undamaged configuration C_0 can be considered representative of the dynamic properties of both specimens. The first natural frequency for the configuration C_1 is also not reported in Table 2 due to some disturbances

ha eliminato: Table 2

ha eliminato: Table 2

affecting the measurements that prevented a clear identification of the fundamental frequency.

Table 2 – Seismic damage: experimental natural frequencies

Configuration	Specimen	Fundamental Frequency - Weak direction	Fundamental Frequency - Strong direction
C_0	B	31.9 Hz	49.5 Hz
C_1	A	N.D.	26.3 Hz
C_2	B	17.9 Hz	28.2 Hz

It is possible to observe that the damage along the strong direction (corresponding to the second mode of vibration) of the column C_1 has a significant impact on the natural frequency with respect to the undamaged condition C_0, resulting in 47% frequency reduction. A similar frequency reduction (44%) is achieved also for the column damaged along the weak direction (C_2) with respect to the undamaged natural frequency in the same direction. Furthermore, for test C_2 is also possible to compute the variation in fundamental frequency along the strong direction due to damage occurred in the weak one, corresponding to a frequency reduction of 43%.

Corresponding mode shapes before and after damage were also analysed, and the CoMAC and Enhanced CoMAC (ECoMAC) indices were computed. Such indices provide a measure of the correlation (CoMAC) or of the average scatter (ECoMAC) of modal displacements at a given position. The CoMAC (Lieven & Ewins, 1988) ranges between 0 and 1, where 1 indicating a perfect correlation (no changes between the compared mode shapes). Conversely, a value of 0 for the ECoMAC (Hunt, 1992) means that the modal displacement of interest remained unchanged for the considered modes in the two datasets under comparison. In the case of real-valued mode shapes and a set of

N_m couples of paired experimental mode shapes, the CoMAC associated with the r-th DOF can be computed as follows:

$$CoMAC_r = \frac{\sum_{s=1}^{N_m} \left| \phi_{r,s}^{und} \cdot \phi_{r,s}^{dam} \right|^2}{\sum_{s=1}^{N_m} \left(\phi_{r,s}^{und} \right)^2 \cdot \sum_{s=1}^{N_m} \left(\phi_{r,s}^{dam} \right)^2} \quad (4)$$

Where $\phi_{r,s}^{und}$ and $\phi_{r,s}^{dam}$ denote the r-th component of the s-th mode shape in the undamaged and damaged condition, respectively.

The ECoMAC associated with the r-th DOF can be instead computed as follows:

$$ECoMAC_r = \frac{\sum_{s=1}^{N_m} \left| \phi_{r,s}^{und} - \phi_{r,s}^{dam} \right|}{2 \cdot N_m} \quad (5)$$

With the same meanings for the symbols. Experimental results show that mode shapes before and after damage are very similar to each other, meaning a minor influence of the considered damage scenario on the fundamental mode shapes of columns and related CoMAC and ECoMAC, as depicted in Fig.6 for test C_2, along the weak direction. In detail, the CoMAC is equal to 1 for all the monitored points, indicating that no significant variations occurred in the mode shapes before and after damage. Similarly, the ECoMAC values are close to 0 at each control point, with only minor variations close to the base of the column, where the potential plastic hinge zone is located. The experimental results attest a slight sensitivity of both indices to the simulated damage, probably due to the limited extent of concrete deterioration. However, given the limited amount of experimental data, such observation needs to be further explored on an enlarged dataset of piers.

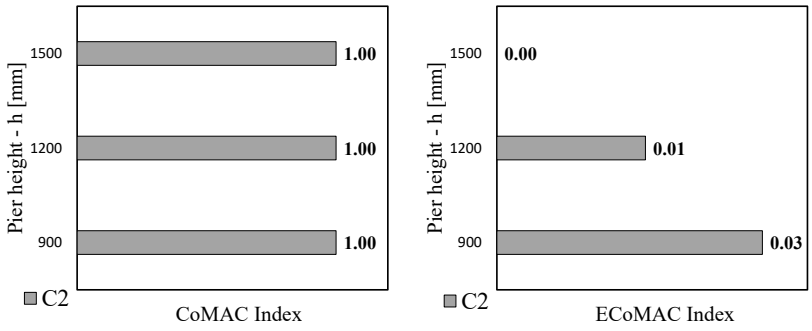

a) b)

Figure 5. COMAC (a) and ECOMAC (b) for each control point of test C_2

4. Numerical modelling

Numerical analyses of the tested specimens and a model updating process have been carried out in order to reliably predict the effect of seismic damage on the fundamental modal properties of RC piers. Several numerical models have been developed to catch the cyclic behaviour of RC piers (Zhang et al. 2021, Bao et al 2023, among many others). In this study, the nonlinear behaviour of column-type elements has been modelled in OpenSees (McKenna et al., 2000) through a distributed plasticity model. The input parameters required for the numerical modelling have been then updated based on the results of the experimental tests, so that a validated baseline for probabilistic analyses has been set. The present study focuses on ductile piers governed by a flexural failure mode; however, the approach can be extended to other typical failure mechanisms (i.e., short piers or piers with lap-splicing) if experimental data for model calibration and validation are available to ensure the reliability of numerical simulations. The BeamWithHinges command is used to build a forceBeamColumn element, which allows distributed plasticity to be spread also beyond the plastic hinge region. For the cantilever

column-type element, a single hinge is defined at the base section, and its length is computed as follows (Paulay & Priestly, 1992):

$$L_{pl} = 0.08\, L_s + 0.022 f_{ym} d_b \quad (2)$$

where Ls is the shear length, d_b the longitudinal bars diameter, and f_{ym} the average yield strength of steel. The solid cross-section of the beam-column element is uniformly discretised into 30 fibres to closely represent small stress-strain variations. The concrete nonlinear behaviour is simulated with the Concrete01 material, which implements the Kent-Scott-Park stress-strain model (D. Kent & R. Park, 1964), while the longitudinal steel reinforcement is modelled with the uniaxial Hysteretic material. The parameters adopted for both stress-strain models are calibrated against experimental data, as discussed in detail in the next section. The fixed-end rotation due to bond slip resulting from strain penetration effects is modelled using a zero-length section element at the end of the beam-column element. The Bond_SP01 material is assigned to the steel fibres of the zero-length section element for taking into account the cyclic bond slip law proposed by Zhao & Sritharan (2007). For the material parameters definition, the yield slip s_y is determined as follows:

$$s_y(mm) = 2.54 \left(\frac{d_b(mm)}{8437} \frac{f_{ym}(MPa)}{\sqrt{f_{cm}}\,(MPa)} (2\alpha + 1) \right)^{1/\alpha} + 0.34 \quad (3)$$

where f_{cm} is the average compressive strength of concrete, and α is taken as 0.4 in accordance with the CEB-FIB Model Code 2010. The ultimate slip s_u is taken as $40 \cdot s_y$, the initial hardening ratio is assumed equal to 0.4 and the pinching factor is 0.6. A fixed restraint is adopted at the base node to simulate the foundation. Geometric nonlinearities are considered in the model by means of the PDelta geometric

ha eliminato: CEB-FIB Model Code 2010

ha formattato: Non Evidenziato

transformation. The Newton-Raphson solution algorithm is adopted to solve the model nonlinear equations. The FE model has first been calibrated against the results of quasi-static cyclic tests. To perform a robust calibration, the results of the quasi-static cyclic tests have been complemented with six additional tests on similar structural elements collected from the literature and presented in Di Ludovico et al. (2014). Hence, the results of eight experimental tests on cantilever RC columns subjected to constant axial load and cyclic quasi-static lateral loads have been employed for model calibration and validation. Geometrical and mechanical properties of the selected columns are summarized in Table 3 along with the constant axial load adopted during the tests. Square as well as rectangular columns, reinforced either with plain or deformed bars, were considered. All the columns were tested following the cyclic load protocol reported in Di Ludovico et al. (2014) which consists in three repetitions for each imposed top displacement, and the observed failure mode was in each case controlled by flexure.

ha eliminato: Table 3

ha formattato: Tipo di carattere: 12 pt

Table 3. Geometric and mechanical parameters of the RC columns for model calibration.

Reference Specimen	**R300P-c**	**R500P-c**	**S300P-c**	**R300D-c**	**R500D-c**	**S300D-c**	**A**	**B**
b (mm)	500	300	300	500	300	300	300	500
h (mm)	300	500	300	300	500	300	500	300
f_{cm} (MPa)	18.8	18.8	18.8	18.8	18.8	18.8	28.8	28.8
f_{ym} (MPa)	*330*	*330*	*330*	*520*	*520*	*520*	*330*	*330*
N (kN)	*282*	*282*	*282*	*282*	*282*	*282*	*428*	*428*
Type of bars	*plain*	*plain*	*plain*	*deformed*	*deformed*	*deformed*	*plain*	*plain*

Formattato: Interlinea: singola

Formattato: Interlinea: multipla 1.15 ri

Formattato: Interlinea: multipla 1.15 ri

Formattato: Interlinea: multipla 1.15 ri

Formattato: Interlinea: multipla 1.15 ri

Formattato: Interlinea: multipla 1.15 ri

Formattato: Interlinea: multipla 1.15 ri

The Young's Modulus of concrete, expressed by means of the concrete strain at maximum strength (f_c) in the *Concrete01* material has been updated in order to achieve

a good agreement between numerical and experimental lateral stiffness and, hence, natural frequency. The model calibration is then performed by updating for each test the concrete strain at peak stress, ε_c, with a step size of 0.001. Figure 6 shows the comparison between experimental and numerical capacity curves along with the value of ε_c that best fits the experimental data. The calibrated values of ε_c range from 0.003 to 0.008 for the selected quasi-static experimental tests. The numerical model reproduces with a satisfactory accuracy key aspects of the experimental response and in particular, the strength, the lateral stiffness and the pinching effect of the specimens at the first repetition of each loading cycle and so doing it confirms the ability in tracking the structural degradation due to damage caused by progressively increasing displacement demand.

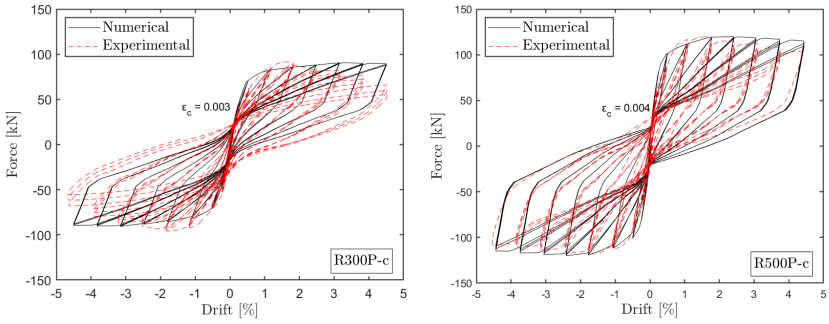

(a) (b)

ha eliminato: ƒ

ha eliminato: Figure 6

ha formattato: Tipo di carattere: 12 pt

ha eliminato: It is noted that the

ha eliminato: s

ha eliminato: a

ha eliminato: reproduces with a reasonable goodacceptable accuracy adopted allows to predict with reasonable accuracy

ha eliminato: ,

ha formattato: Non Evidenziato

ha eliminato: catching the

ha eliminato: It is also observed that the numerical curves fit quite well the hysteretic behaviour of the RC columns in terms of peak strength, lateral stiffness, and pinching effect, well catching the degradation due to damage.

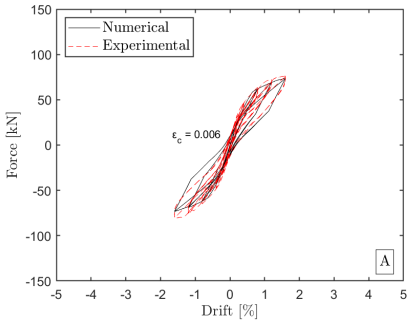
Numerical
Experimental
ε_c = 0.006
A
Force [kN]
Drift [%]

(c)

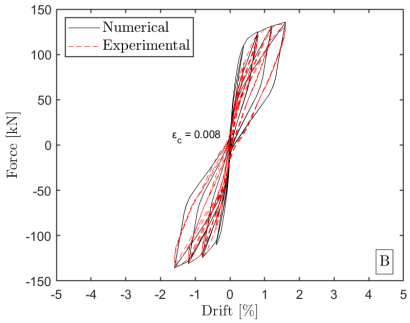
Numerical
Experimental
ε_c = 0.008
B
Force [kN]
Drift [%]

(d)

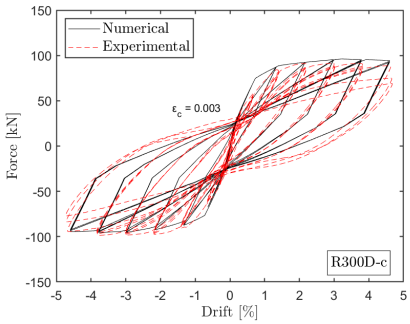
Numerical
Experimental
ε_c = 0.003
R300D-c
Force [kN]
Drift [%]

(e)

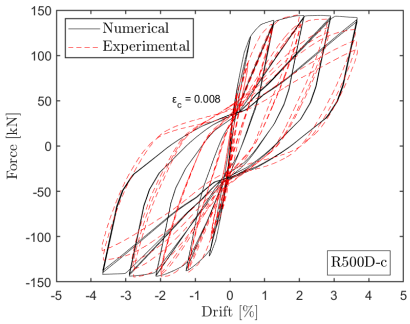
Numerical
Experimental
ε_c = 0.008
R500D-c
Force [kN]
Drift [%]

(f)

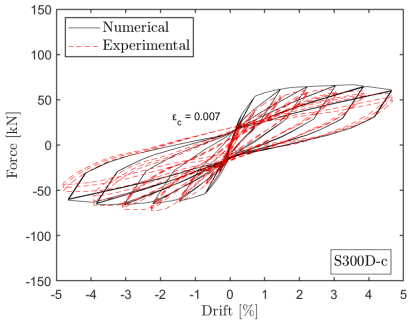
Numerical
Experimental
ε_c = 0.007
S300D-c
Force [kN]
Drift [%]

(g)

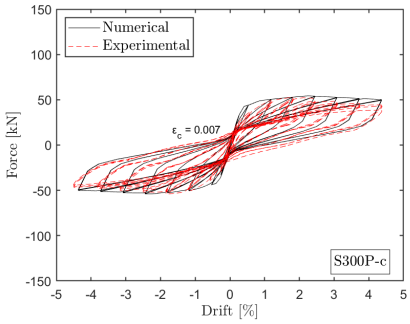
Numerical
Experimental
ε_c = 0.007
S300P-c
Force [kN]
Drift [%]

(h)

Figure 6. Comparison between numerical and experimental capacity curves for the selected eight tests.

The resulting calibrated models have been then validated against results of output-only modal identification tests in the undamaged and damaged configurations. To this aim, the experimental frequencies of configurations C_0, C_1 and C_2 (reported in Table 2) have been compared with those obtained from *OpenSees* before and after the non-linear static cyclic analysis. Indeed, the *OpenSees* software updates the stiffness matrix of the model to account for the damage occurred during the cyclic loading and modifies the results of the modal analysis. The comparison of natural frequencies is reported in Table 4, along with the value of ε_c associated with the minimum error between experimental and numerical frequencies. It can be noted that for specimen B, a value of ε_c ranging from 0.005 to 0.006 provides the lowest error in terms of natural frequencies for both configurations C_0 and C_2. The same value of ε_c = 0.006 is found to best fit the hysteretic curve from quasi-static test (Figure 6(c)). Similarly, a value of ε_c =0.008 has been found to provide a good match both with the static and dynamic behaviour of specimen A (Figure 6(d)). The consistency of the obtained results confirms that the FE model is able to predict with a good accuracy the static and dynamic response of column-type elements in both the undamaged and seismically damaged configurations for the considered failure mode.

ha formattato: Tipo di carattere:
ha eliminato: Table 2
ha formattato: Tipo di carattere:
ha eliminato: Table 4
ha eliminato: Figure 6
ha formattato: Tipo di carattere: 12 pt
ha eliminato: Figure 6
ha formattato: Tipo di carattere: 12 pt

Table 4. Comparison between experimental and numerical natural frequencies.

Configuration	**Specimen**	**Fundamental frequency Weak direction**			**Fundamental frequency Strong direction**		
		Experimental	*OpenSees*	ε_c	Experimental	*OpenSees*	ε_c
C_0	B	31.9 Hz	30.8 Hz	0.005	49.5 Hz	50.1 Hz	0.005
C_1	A	-	-	-	28.2 Hz	28.4 Hz	0.008
C_2	B	17.3 Hz	17.3 Hz	0.006	-	-	-

Formattato: Interlinea: singola

5. Correlating modal-based damage features and seismic damage level

A correlation between variations in modal-based features of RC bridge piers (i.e., natural frequency, CoMAC and ECoMAC) and seismic damage levels is numerically assessed adopting a probabilistic approach. A portfolio of 200 cantilever RC piers with a rectangular solid cross-section has been generated through Monte Carlo simulation, and extensive numerical analyses have been carried out adopting the validated FE model.

The definition of the RC bridge piers dataset relies on the Latin Hypercube sampling technique and adopts data distributions from the extensive study performed by Zelaschi et al. (2016) to characterize the portfolio of existing Italian bridges (1970s-1990s). As mentioned before, this study focuses on simply supported bridges following the schematic representation of Figure 7. Structural scheme of examined bridge and loading scheme: longitudinal profile (a) and transverse profile (b).

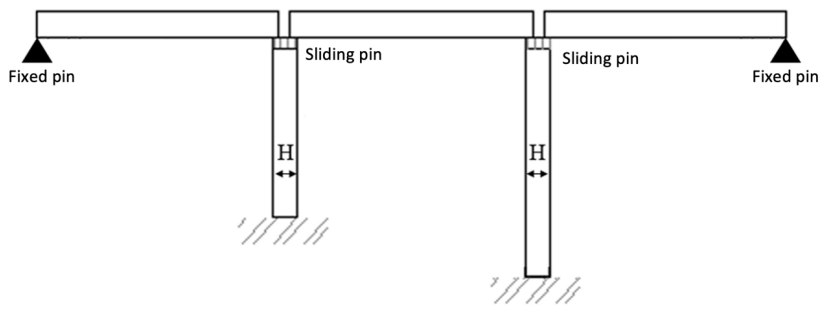

(a)

ha formattato: Controllo ortografia e grammatica

ha eliminato: Figure 7. Structural scheme of examined bridge and loading scheme: longitudinal profile (a) and transverse profile (b). The simulation considers an earthquake occurring in the transverse direction of the bridge, so as the seismic behaviour of the pier can be approximated to a cantilever.¶

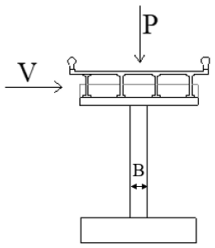

(b)

Figure 7. Structural scheme of examined bridge and loading scheme: longitudinal profile (a) and transverse profile (b).

Relevant geometrical and mechanical properties collected from a real stock of about 458 Italian RC bridges presented in Zelaschi et al. (2016) are summarized in Table 5. In particular, the type of distribution along with relevant statistics are reported for pier height (h), pier cross section dimensions (B and H, as reported in Figure 7), steel and concrete mean strength (f_{ym} and f_{cm}). It should be noted that the pier always presents the strong axis in the transverse direction of the bridge. For the steel reinforcement ratio (ρ), a uniform distribution is adopted in the range 0.5%-1.0% (Perdomo & Monteiro, 2021). The concrete stiffness is also taken as random variable for the Monte Carlo simulation, randomly selecting the concrete strain at maximum strength of the Concrete01 material in the range 0.003-0.008, based on the outcomes of the model calibration discussed in Section 4. The distributions of geometrical and mechanical properties for the generated sample of 200 RC piers are plotted in Figure 8.

ha formattato: Tipo di carattere:

ha eliminato: Table 5

ha eliminato: Figure 7

ha formattato: Tipo di carattere: Non Grassetto, Controllo ortografia e grammatica

ha eliminato: Figure 8

ha formattato: Tipo di carattere:

Table 5. Statistics of relevant geometrical and mechanical properties of existing bridge piers (Zelaschi et al., 2016).

Variable	Distribution	Distribution parameters
Pier height (h) [m]	Lognormal	Mean (log): 1.95

		std.: 0.8275
Solid rectangular section – dimension in the bridge transverse direction (B) [m]	Weibull	Shape: 1.65 Scale: 2.34
Solid rectangular section – dimension in the bridge longitudinal direction (H) [m]	Weibull	Shape: 0.96 Scale: 2.79
Steel tensile strength (f_{ym}) [MPa]	Normal	Mean: 504.40 std.: 157.84
Concrete compressive strength (f_{cm}) [MPa]	Normal	Mean: 40.00 std.: 7.44
Average span length [m]	Normal	Mean: 29.936 std: 12.174
Superstructure area [m^2]	Lognormal	Mean (log): 7.88 std: 0.9087

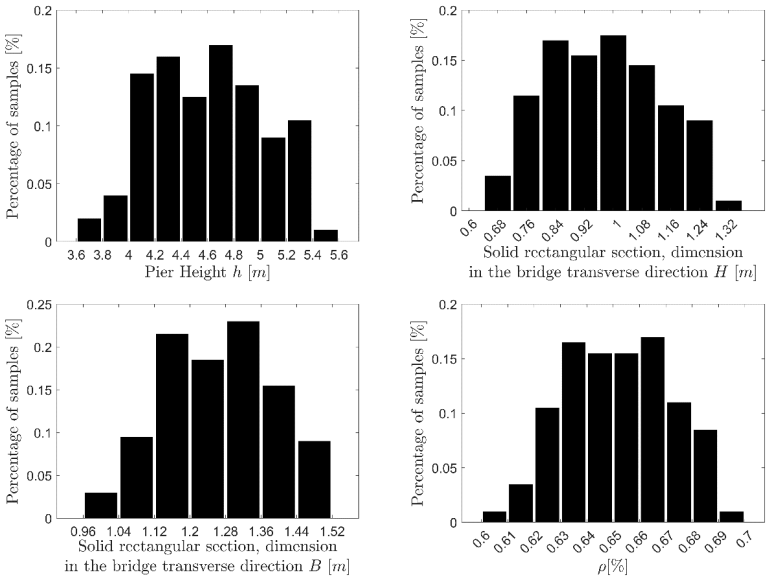

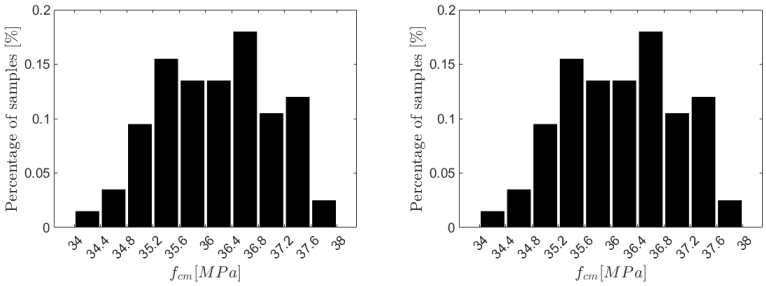

Figure 8. Distribution of geometrical and mechanical parameters for the population of 200 RC bridge piers (Zelaschi et al., 2016)

The mass of the bridge deck is computed based on the distribution of the superstructure area and of the average span length (Zelaschi et al., 2016), both treated as random variables in the Monte Carlo simulation and reported in Table 5. The tributary mass assigned to the generic bridge pier is then computed multiplying the superstructure area, the span length and the typical density of reinforced concrete (i.e., 25 kN/m^3). The tributary mass is concentrated at the top node of the cantilever pier in the *OpenSees* model. The general framework adopted for the numerical simulations is depicted in Figure 9 (Lubrano Lobianco et al., 2021). Once the refined numerical model is built for the generic pier, the fundamental modal properties of the model are obtained by numerical modal analysis in the undamaged condition. A cyclic loading path under displacement control analysis is performed to simulate the seismic damage associated with an imposed drift ratio (DR) in the transverse direction of the bridge; at this stage the variation in the modal properties induced by damage is evaluated by repeating the modal analysis. The sequential cyclic loading-modal analyses are repeated for six imposed DRs for all the piers in the portfolio. The overall procedure is described in Figure 9, which also shows the cyclic loading sequence adopted to determine an increased inelastic demand on the base section. This way of approaching the problem complies a well-established technical literature on the experimental characterization of the rotation capacity of RC. members

ha eliminato: Table 5

ha eliminato: Figure 9

ha formattato: Tipo di carattere: Non Grassetto, Controllo ortografia e grammatica

ha eliminato: Figure 9

ha formattato: Tipo di carattere: Non Grassetto, Controllo ortografia e grammatica

subjected to earthquake loading. The load protocol with three repetitions at increasing drift ratio levels, indeed, was originally introduced by Krawlinker (1996) and included in the ATC-24 guidelines (1992), and it has been extensively used in the reinforced concrete experimental research (Biskinis et al., 2010). On this subject, it is worth noting that such an approach fits the objectives and above all the main structural and dynamical features of the investigated members, whose moderate to low slenderness clearly suggests that higher modes do not affect the response under seismic actions, and avoids any manipulation of the seismic dynamic input to control the DR level.

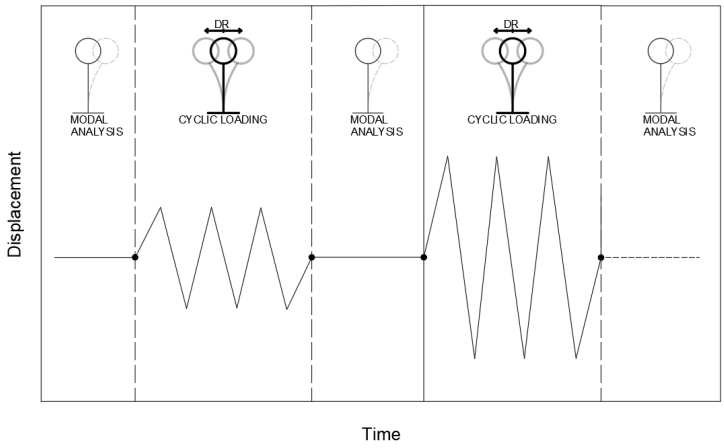

Figure 9. Methodological framework for seismic damage quantification through numerical simulations.

The details of the load protocol is reported in Table 6 in terms of imposed DR and number of repetitions for each cycle up to a DR=4.8%, which is assumed to represent a limit value for the complete damage of the pier. A constant axial load ratio equal to 0.1 is applied in the model during the numerical cyclic loading analyses.

Table 6 – Lateral load protocol adopted for the numerical simulations.

Loading sequence	*DR* [%]	Number of repetitions for each cycle
I	0.80	3
II	1.20	3
III	1.60	3
IV	2.40	3
V	3.20	3
VI	4.80	3

For each cyclic loading phase, the damage level is assessed by computing the P&A DI on the hysteretic capacity curve. To assess the DI at each imposed DR, the ultimate rotation capacity of the piers is computed as reported in Perdomo and Monteiro (2021). Then, the variation of the modal-based damage features is assessed and correlated with the damage level experienced by the pier according to the seismic damage scale reported in Table 1. Given the number of DR investigated, a total of 1200 data are collected from the numerical simulations. Natural frequencies variation in the loading direction are denoted in the following as Δf_1. The plot in Figure 10 shows the probability distributions of Δf_1 for the set of simulations as a function of the imposed DR. It is clear from numerical results the effect of increasing seismic demand, expressed by means of the displacement demand, on the variation of natural frequency for the piers.

ha eliminato: Table 1

ha formattato: Tipo di carattere: 12 pt

ha eliminato: Figure 10

ha formattato: Tipo di carattere: Non Grassetto, Controllo ortografia e grammatica

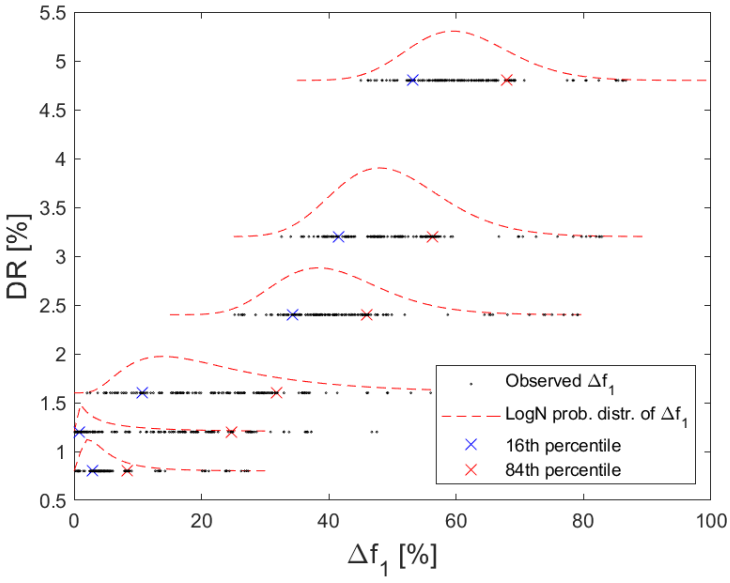

Figure 10. Probability distribution of Δf_1 as a function of the DR for the portfolio of 200 piers.

Each simulation has been paired with the associated P&A damage level, as depicted in Figure 11(a). Among the dataset of 1200 simulations, 200 (16%) reached a DS1, 400 (32%) a DS2, 400 (32%) a DS3 and 200 (16%) a DS4, thus ensuring a sufficient number of data for each damage level. Figure 11(b) shows the number of simulations that reached a certain variation of fundamental frequency, Δf_1, for each damage level. For DS1, most of the simulations showed a frequency variation lower than 10%, whereas frequency variations ranging between 10-30% are observed for the simulations classified as DS2. For DS3 variation of natural frequency ranges between 30% to 80%, with higher number of data in the range 40-60%. Similarly, for DS4 the frequency variation is between 50% and 100%, with a higher density of results in the range 60-80%.

ha eliminato: Figure 11

ha eliminato: Figure 11

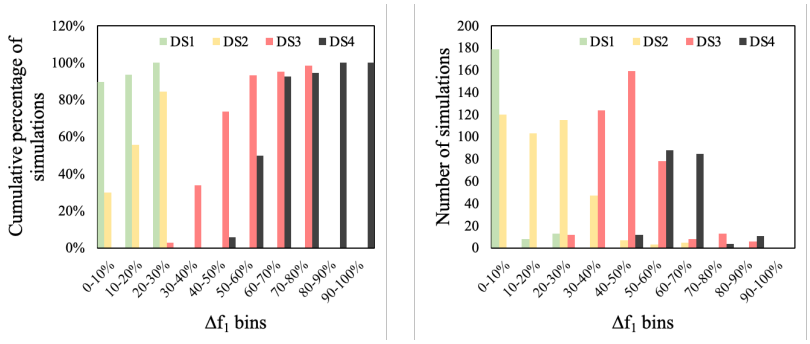

(a) (b)

Figure 11. Cumulative distribution of simulations for each DS (a), and frequency distribution for each DS (b) as a function of Δf_1.

To finally provide information about the probability of occurrence of a certain DS given an observed variation of natural frequency in the monitored pier, a fragility model in the form of lognormal cumulative probability functions is derived from the results of numerical simulations, as plotted in Figure 12. In the Figure, both the cumulative distributions of numerical data and the fitted lognormal curves are reported for each damage level. The fitting is herein performed adopting the Least Square Estimation method. Mean (μ) and logarithmic standard deviation (β) for the derived curves are reported in Table 6. The fragility curves allow to assess in a probabilistic framework the correlation of a variation in fundamental frequency due to structural damage in the pier and the probability of occurrence of a certain damage level. For instance, a frequency variation of 40% with respect to the reference condition can be associated with a probability of occurrence of 100% of DL1, 90% of DL2, 28% of DL3 and 0% of DL4. Such kind of information can support decision making processes about serviceability of bridges in the aftermath of an earthquake. Furthermore, additional sources of uncertainties such as environmental effects can be included in the probabilistic model to

ha eliminato: Figure 12

ha formattato: Tipo di carattere:

ha formattato: Tipo di carattere: Non Grassetto, Controllo ortografia e grammatica

ha eliminato: Table 6

update the curves based on real observations of the frequency variation over time of the monitored assets in the undamaged reference configuration.

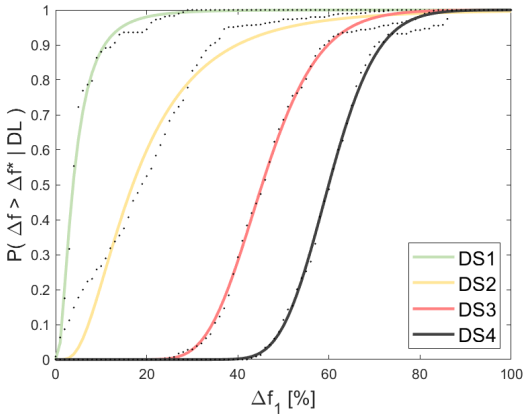

Figure 12. Probability of exceedance of each DS as a function of Δf_1.

Table 6. Frequency variation probability functions parameters (μ [log] and β) for each damage level

Damage state	μ [%]	β [-]
DS1	4.4	0.80
DS2	16.0	0.67
DS3	49.3	0.22
DS4	60.3	0.14

While the previous results confirm the sensitivity of the fundamental natural frequencies to damage, the corresponding mode shapes appear less sensitive to seismic damage intensity. To compute the CoMAC and ECoMAC indices related to numerically computed mode-shapes at different stages of analysis and, therefore, damage levels, three

control points are adopted. For each column, their distance from the base section, normalized with respect to the pier height H, is 0.3, 0.5 and 0.7. However, it is expected to have more significant variations of both indices near the pier base where the seismic damage is concentrated (i.e., plastic hinge region). The mean, the 16th and the 84th percentiles of the distributions of CoMAC and ECoMAC obtained from numerical simulations for different damage levels are depicted in Figure 13(a) and Figure 13(b), respectively, for the control point at 0.3 from the base of the piers, which is located in the potential plastic hinge region. The figures show that both CoMAC and ECoMAC are slightly sensitive to the simulated seismic damage. Similar results are obtained for the other control points for which the plots of CoMAC and ECoMAC are not herein reported for the sake of brevity. The numerical analyses also confirm that the fundamental mode shapes are not very sensitive to the considered seismic damage scenario, in agreement with the experimental observations reported in Section 3.2. Comparing the two damage

ha eliminato: Figure 13

ha eliminato: Figure 13

indices, the ECoMAC appears to be slightly more sensitive than the CoMAC in detecting and localising seismic damage.

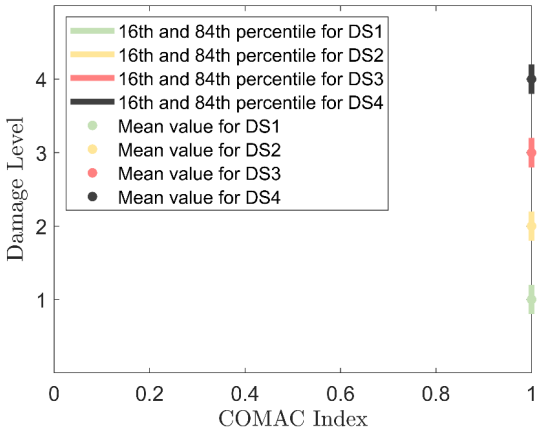

(a)

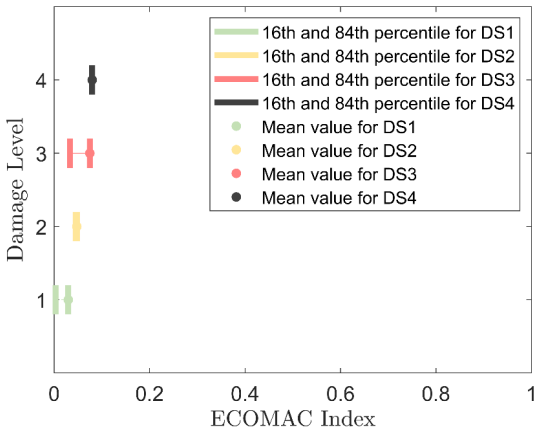

(b)

Figure 13. COMAC (a) and ECOMAC (b) for control point at 0.3H from the base of the pier.

6. Conclusions

The present paper proposed an approach for the probabilistic seismic damage assessment in simply supported bridge RC piers through the fast interpretation of data from vibration-based SHM. The study reports the main results of extensive numerical simulations to evaluate variations in modal-based properties (i.e., natural frequency, CoMAC and ECoMAC) of RC piers as a function of the experienced seismic damage. A refined FE model, calibrated over original experimental results of column-type RC members subjected to quasi-static lateral loading and to sequential output-only modal identification tests at different drift ratio levels, has been developed in *OpenSees*. The validated model has been used to perform extensive probabilistic analyses over a portfolio of 200 rectangular RC piers with solid cross-section, representative of existing piers in Italian road bridges. A seismic damage level classification has been proposed to correlate the observed variations in modal-based properties of piers with the seismic damage experienced by the piers.

The main outcomes of the present study can be summarized as follows:

- The proposed simulation workflow demonstrated its ability in relating the variation in natural frequencies to the seismic cyclic displacement demand on RC piers, and its potential in providing similar results once its application is extended and verified with reference to different piers types and more complex bridge types;
- Seismic damage mainly affected the fundamental natural frequencies of the piers belonging to the investigated bridge layouts, while the mode shapes were less sensitive to the simulated structural damage. Hence, the natural frequencies are the primary damage sensitive parameter to be observed when the characterization and estimation of the seismic damage through vibration-based SHM systems is of interest;
- Original fragility functions relating the observed variation of fundamental frequency with the probability of exceedance of given damage levels has been

ha eliminato: an

ha eliminato:

ha eliminato: *s*

ha eliminato: .

ha eliminato: adopted

ha eliminato: Based on the presented outcomes, the following findings can be highlighted

ha formattato: Tipo di carattere: 12 pt

ha formattato: Tipo di carattere: 12 pt

ha eliminato: proposed numerical framework and FE modelling approach are able to well describing

ha eliminato: the catch the

ha eliminato: due

ha eliminato: to

ha eliminato: induced

ha eliminato:

ha eliminato: and, hence, can be adopted for future numerical studies onfurther developed in order to extend its application to different

ha eliminato: (expressed through the indices CoMAC and ECoMAC)

ha eliminato: estimate

ha eliminato: the use of

ha eliminato: to quantify and estimate the seismic damage through vibration-based SHM systems

ha eliminato: is

ha eliminato: suggested

ha eliminato: advisable

ha formattato: Tipo di carattere:

ha eliminato: AFor probabilistic damage assessment in the aftermath of an earthquake, fragility functions related to the variation of fundamental frequencies of piers for different damage levels can be adopted. n o

derived and presented with the aim of offering rational tools for the operation of vibration based structural monitoring and consequent decision making in the aftermath of an earthquake;

- The cost of the SHM system for simply supported RC bridges with ductile piers can be optimized by installing sensors only on top of the piers to track the variations of fundamental frequencies.

Further work is needed to increase the overall reliability of the results, extending them to different failure modes (i.e., shear, lap-splice) and structural systems to provide a comprehensive probabilistic framework for damage detection and quantification through SHM vibration data.

Acknowledgments

The present study has been carried out in the framework of the PRIN 20172 LHSEA Research Project, whose financial support is gratefully acknowledged. This work is also part of the research activity developed by some of the authors within the framework of the "PNRR": SPOKE 7 "CCAM, Connected Networks and Smart Infrastructure" - WP4. Additional support from the Superior Council of Public Works and RELUIS in the framework of the WP3 Analysis, revision and update of Guidelines is also gratefully acknowledged. The Authors would also finally acknowledge the contribution of S2X s.r.l., which provided the software for dynamic data acquisition (https://www.s2x.it/s2-dda/) and remote technical support during the OMA tests.

References

Allemang, R. J., & Brown, D. L. (1982). A correlation coefficient for modal vector analysis, Proceedings of the first international Modal Analysis Conference. *Sdrl.Uc.Edu*, 110–116.

Applied Technology Council (ATC). (1992). Guidelines for cyclic seismic testing of components of steel structures. ATC-24.

Bao, L., Zhao, J., Teng, F., Bao, Y., Zhao, T., & Yu, L. (2023, June). Experimental study on the seismic performance of prefabricated frame piers. In Structures (Vol. 52, pp. 651-

ha formattato: Tipo di carattere:

ha spostato (inserimento) [1]

ha eliminato: <#>The functions correlate an observed variation of fundamental frequency with the probability of occurrence of different damage levels. The results reported in this paper, i.e. parameters of the fragility functions, can be used to set appropriate threshold values for planning maintenance activities or for the rapid assessment of the serviceability of monitored road bridges;¶

ha eliminato: <#>study also attested that the

ha eliminato: <#>s

ha formattato: Tipo di carattere: 12 pt

ha spostato in alto [1]: The study also attested that the costs of the SHM system for simply supported RC bridges with ductile piers can be optimized by installing sensors only on top of the piers to track the variations of fundamental frequencies.

ha eliminato: ¶

ha eliminato: More in detail, original tests on two cantilever RC columns are herein presented and adopted for model calibration and validation. The collected data have been complemented with others 6 tests available from the literature and used for the calibration and validation of a numerical model able to predict the seismic performance of ductile piers governed by a flexural failure mode. ¶
The validated model has been adopted to perform extensive probabilistic analyses over a portfolio of 200 rectangular RC piers with solid cross-section, representative of existing piers in Italian road bridges. Seismic damage has been simulated through non-linear static pushover analysis for increasing imposed drift ratios. A seismic damage level classification has been adopted to correlate the numerically observed variations in modal-based properties of piers with the seismic damage experienced during the simulation. Numerical results have shown that seismic damage mainly affected the fundamental natural frequencies of the piers, while the mode shapes (expressed through the indices CoMAC and ECoMAC) were less sensitive to estimate the simulated structural damage. Hence, the use of natural frequencies to quantify and estimate the damage through vibration-based SHM systems is suggested. For probabilistic damage assessment in the aftermath of an earthquake, fragility functions related to the variation of fundamental frequencies of piers for different damage levels were proposed. The functions correlate an observed variation of fundamental frequency with the probability of occurrence of different damage levels. The proposed functions can be adopted to set appropriate threshold values for planning maintenance activities or for the rapid assessment of the serviceability of monitored road bridges. ¶

ha eliminato: wider

665).Biskinis, D., & Fardis, M. N. (2010). Flexure-controlled ultimate deformations of members with continuous or lap-spliced bars. Structural concrete, 11(2), 93-108.

Brincker, R., & Ventura, C. E. (2015). Introduction to Operational Modal Analysis. *Introduction to Operational Modal Analysis*, 1–360. https://doi.org/10.1002/9781118535141

D. Kent, & R. Park. (1964). Flexural Members with Confined Concrete. *Journal of the Structural Division*, *97*, 1969–1990.

Del Zoppo, M., Di Ludovico, M., Balsamo, A., & Prota, A. (2018). Comparative analysis of existing RC columns jacketed with CFRP or FRCC. *Polymers*, *10*(4). https://doi.org/10.3390/polym10040361

Di Ludovico, M., Verderame, G. M., Prota, A., Manfredi, G., & Cosenza, E. (2014a). Cyclic Behavior of Nonconforming Full-Scale RC Columns. *Journal of Structural Engineering*, *140*(5). https://doi.org/10.1061/(asce)st.1943-541x.0000891

Di Ludovico, M., Verderame, G. M., Prota, A., Manfredi, G., & Cosenza, E. (2014b). Cyclic Behavior of Nonconforming Full-Scale RC Columns. *Journal of Structural Engineering*, *140*(5). https://doi.org/10.1061/(asce)st.1943-541x.0000891

fib Bulletins 65-66 (2010), Model code 2010 Final Draft, 2010. fédération internationale du béton (fib), Lausanne (Switzerland).

Foti, D. (2013). Dynamic Identification Techniques to Numerically Detect the Structural Damage. *The Open Construction and Building Technology Journal*, *7*(1), 43–50. https://doi.org/10.2174/1874836801307010043

Fujino, Y., & Siringoringo, D. M. (2008). Structural health monitoring of bridges in japan: An overview of the current trend. *Proceedings of the 4th International Conference on FRP Composites in Civil Engineering, CICE 2008*.

Hunt D.L., Application of an enhanced coordinate modal assurance criterion (ECOMAC), IMAC 1992, 66–71

Hurt, M., & Schrock, S. D. (2016). Highway Bridge Maintenance Planning and Scheduling. In *Highway Bridge Maintenance Planning and Scheduling*. https://doi.org/10.1016/C2014-0-01037-4

Jin, C., Jang, S., Sun, X., Li, J., & Christenson, R. (2016). Damage detection of a highway bridge under severe temperature changes using extended Kalman filter trained neural network. *Journal of Civil Structural Health Monitoring*, *6*(3), 545–560. https://doi.org/10.1007/s13349-016-0173-8

Hernandez Jr, J., Miyashita, T., Ishii, H., Vorabouth, P., & Fujino, Y. (2006). Identification of modal characteristics of shinkansen RC viaducts using laser doppler vibrometers.

Junwon, S., Jong, W., & Jaeha, L. (2015). Summary Review of Structural Health Monitoring Applications for Highway Bridges. *Journal of Performance of Constructed Facilities*, *26*(4), 371–376.

Kariyawasam, K. D., Middleton, C. R., Madabhushi, G., Haigh, S. K., & Talbot, J. P. (2020). Assessment of bridge natural frequency as an indicator of scour using centrifuge modelling. *Journal of Civil Structural Health Monitoring*, *10*(5), 861–881. https://doi.org/10.1007/s13349-020-00420-5

Krawinkler, H. (1996). Cyclic loading histories for seismic experimentation on structural components. Earthquake Spectra, 12(1), 1-12.

Lieven N. A.J., Ewins D.J., Spatial correlation of mode shapes, The coordinate modal assurance criterion (COMAC), IMAC 1988,690–695

Limongelli, M. P., & Giordano, P. F. (2020). Vibration-based damage indicators: a comparison based on information entropy. *Journal of Civil Structural Health Monitoring*, *10*(2), 251–266. https://doi.org/10.1007/s13349-020-00381-9

Londono, N. A. (2006). *Use of vibration data for structural health monitoring of bridges*. 1–243.

Lubrano Lobianco, A., Del Zoppo, M., & Di Ludovico, M. (2021). Seismic Damage Quantification for the SHM of Existing RC Structures. *Lecture Notes in Civil Engineering*, *156*, 177–195. https://doi.org/10.1007/978-3-030-74258-4_12

Magalhães, F., Cunha, A., & Caetano, E. (2012). Vibration based structural health monitoring of an arch bridge: From automated OMA to damage detection. *Mechanical Systems and Signal Processing*, *28*, 212–228. https://doi.org/10.1016/j.ymssp.2011.06.011

Martakis, P., Reuland, Y., Stavridis, A., & Chatzi, E. (2023). Fusing damage-sensitive features and domain adaptation towards robust damage classification in real buildings. Soil Dynamics and Earthquake Engineering, 166, 107739.

McKenna, F., Fenves, G., & Scott, M. (2000). Open system for earthquake engineering simulation. *Pacific Earthquake Engineering Research Center*, 465.

Ministero delle Infrastrutture e dei Trasporti, & Consiglio Superiore Lavori Pubblici. (2020). *Linee Guida per la Classificazione e Gestione del Rischio, la Valutazione della Sicurezza ed il Monitoraggio dei Ponti Esistenti - Allegato D: Schede di ispezione speciale - Ponti in c.a.p. a cavi post-tesi*.

Mirza, K. (2006). Seismic Structural Health Monitoring. *PhD Thesis*, *June*.

Moroni, M. O., Boroschek, R., & Sarrazin, M. (2005). Dynamic Characteristics of Chilean Bridges with Seismic Protection. *Journal of Bridge Engineering*, *10*(2), 124–132. https://doi.org/10.1061/(asce)1084-0702(2005)10:2(124)

Moughty, J. J., & Casas, J. R. (2017). A state of the art review of modal-based damage detection in bridges: Development, challenges, and solutions. *Applied Sciences (Switzerland)*, *7*(5). https://doi.org/10.3390/app7050510

Park, Y., Ang, A. H. -S., & Wen, Y. K. (1985). Seismic Damage Analysis of Reinforced Concrete Buildings. *Journal of Structural Engineering*, *111*(4), 740–757. https://doi.org/10.1061/(asce)0733-9445(1985)111:4(740)

Paulay, T., & Priestly, M. J. N. (1992). Seismic Design of Reinforced Concrete and Masonry Buildings. *Seismic Design of Reinforced Concrete and Masonry Buildings*. https://doi.org/10.1002/9780470172841

Perdomo, C., & Monteiro, R. (2021). Extension of displacement-based simplified procedures to the seismic loss assessment of multi-span RC bridges. *Earthquake Engineering and Structural Dynamics*, *50*(4), 1101–1124. https://doi.org/10.1002/eqe.3389

Priestley, M.J.N., Seible F., Calvi, G. M. (1996). Seismic design and retrofit of bridges. *John Wiley and Sons*.

Promis, G., Ferrier, E., & Hamelin, P. (2009). Effect of external FRP retrofitting on reinforced concrete short columns for seismic strengthening. *Composite Structures*, *88*(3), 367–379. https://doi.org/10.1016/j.compstruct.2008.04.019

Rainieri, C., & Fabbrocino, G. (2014). *Operational Modal Analysis of Civil Engineering Structures: An Introduction and Guide for Applications*. 322.

Rainieri, C., Gargaro, D., Fabbrocino, G., Maddaloni, G., Di Sarno, L., Prota, A., & Manfredi, G. (2018). Shaking table tests for the experimental verification of the effectiveness of an automated modal parameter monitoring system for existing bridges in seismic areas. *Structural Control and Health Monitoring*, *25*(7). https://doi.org/10.1002/stc.2165

Rainieri, C., Magalhaes, F., Gargaro, D., Fabbrocino, G., & Cunha, A. (2019). Predicting the variability of natural frequencies and its causes by Second-Order Blind Identification. *Structural Health Monitoring*, *18*(2), 486–507. https://doi.org/10.1177/1475921718758629

Rainieri, C., Notarangelo, M. A., & Fabbrocino, G. (2020). Experiences of dynamic identification and monitoring of bridges in serviceability conditions and after hazardous events. *Infrastructures*, *5*(10), 1–23. https://doi.org/10.3390/infrastructures5100086

Reynders, E., Wursten, G., & de Roeck, G. (2014). Output-only structural health monitoring in changing environmental conditions by means of nonlinear system identification. *Structural Health Monitoring*, *13*(1), 82–93. https://doi.org/10.1177/1475921713502836

Reuland, Y., Khodaverdian, A., Crowley, H., Nievas, C., Martakis, P., & Chatzi, E. (2023, August). Monitoring-Driven Post-earthquake Building Damage Tagging. In *International Conference on Experimental Vibration Analysis for Civil Engineering Structures* (pp. 550-559). Cham: Springer Nature Switzerland.

Zelaschi, C., Monteiro, R., & Pinho, R. (2016). Parametric Characterization of RC Bridges for Seismic Assessment Purposes. *Structures*, *7*, 14–24. https://doi.org/10.1016/j.istruc.2016.04.003

Zhao, J., & Sritharan, S. (2007). Modeling of strain penetration effects in fiber-based analysis of reinforced concrete structures. *ACI Structural Journal*, *104*(2), 133–141.

Zhang, G., Han, Q., Xu, K., Du, X., & He, W. (2021). Experimental investigation of seismic behavior of UHPC-filled socket precast bridge column-foundation connection with shear keys. Engineering Structures, 228, 111527

Zhelyazkov, A., Zonta, D., Wenzel, H., & Furtner, P. (2020). On the estimation of the ductility demand on reinforced concrete bridge piers from structural health monitoring data. *Journal of Civil Structural Health Monitoring*, *10*(2), 283–295. https://doi.org/10.1007/s13349-020-00383-7